Monte Carlo simulation of photon migration path in turbid media

Jiangang Wang (王建岗), Guiying Wang (王桂英), and Zhizhan Xu (徐至展)

State Key Laboratory of High Field Laser Physics, Shanghai Institute of Optics and Fine Mechanics, Chinese Academy of Sciences, Shanghai 201800

Received October 29, 2007

A new method of Monte Carlo simulation is developed to simulate the photon migration path in a scattering medium after an ultrashort-pulse laser beam comes into the medium. The most probable trajectory of photons at an instant can be obtained with this method. How the photon migration paths are affected by the optical parameters of the scattering medium is analyzed. It is also concluded that the absorption coefficient has no effect on the most probable trajectory of photons.

OCIS codes: 170.7050, 170.5280, 290.0290, 999.9999.

doi: 10.3788/COL20080607.0530.

With much more applications of lasers in disease diagnoses, medical imaging, tomography, etc, a better understanding of the fundamental principles of photon migration in turbid media is important. So many models have been put forward in order to describe the photon behavior in turbid media, for instance, the diffusion approximation[1], the finite element method[2], the discrete lattice model[3], the Monte Carlo method[4−6], etc. Only in the cases of simple geometry and simple boundary conditions the analytical solutions could be obtained. The Monte Carlo method has many uses in solving the practical problems, for its flexibility, its ability to deal with various geometrical and boundary conditions[7,8]. Nowadays the computer has more powerful calculation abilities; in fact, the limit of calculation speed and storage space on the Monte Carlo method has been weakening gradually. The results of Monte Carlo simulations are regarded as a non-experimental standard to verify the other results from other models. We know that the light wave propagated in the turbid media can be seen as photons similar to classical particles, and the photons randomly walk in the media. Despite the photon randomness, there exists the classical path of photons at a specific time[9−14], i.e., the most probable trajectory. The most probable trajectory means that the photon densities on the trajectory have greater values than that of the nearby region. Previous Monte Carlo simulations of photon migration have mainly provided the overall results at the surface of the turbid media, but not the most probable path at some instant.

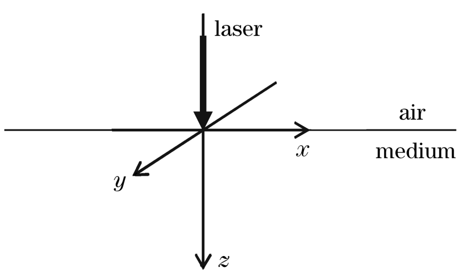

Fig. 1. Geometric configuration and the coordinates.

A cylindrical coordinates system is set up. As shown in Fig. 1, an ultrashort-pulse laser beam is incident on a turbid medium from air at time t_0 with the central axis of the beam coinciding with the z axis. The medium is assumed to occupy the half space of $z \geq 0$ or one slab space with thickness d. It is characterized by a refractive index n, scattering coefficient μ_{s}, anisotropy factor g, absorption coefficient μ_{a}. The ultrashort laser beam can be considered as a δ stimulator under the conditions of our adopted grids of space and time. The space and time are sliced into elements with even separation. The number of grid elements in the r, z, and t coordinates is N_r, N_z, and N_t, respectively. The corresponding grid separation is Δr, Δz, and Δt. Here r is $r = (x^2 + y^2)^{1/2}$.

The Monte Carlo (MC) method simulates the photon migration procedure in the highly scattering medium. The random numbers generated by the random generator decide the walking step and direction of one photon[15,16]. The photon interacts with the medium in every step, i.e., the photon is scattered and absorbed. And its left weight ratio of the photon is defined by the albedo $\mu_{\mathrm{s}}/(\mu_{\mathrm{s}} + \mu_{\mathrm{a}})$. We must trace a large number of photons and the statistical results are of significance. If one photon emits out the surface of the medium or its weight is less than a certain value, we can stop tracing it. The Fresnel reflection coefficient and the Snell's law are used to treat with reflection and refraction of one photon at the index-of-refraction mismatched boundary. We use the time-histogram method to simulate the time dependence of photon migration[15].

How can we get the classical trajectory of the photons reaching the surface of the medium at a specific time? The procedure can be divided into four steps:

1) One photon is launched to be traced by MC method. When the photon stays in one space grid after one random walking, the counting number in the space grid is incremented.

2) If the photon is dead when it satisfies with its termination conditions, we stop tracing the photon. Then if it reaches the surface of the medium, we record the delay time t of the photon from the beginning time t_0 and store the counting numbers in all space grids.

3) We repeat the above steps until a large number of photons are traced. Now the counting number in every space grid at a specific time reflects how many times that the photons reaching the surface pass the space grid. If the counting number is assumed to be $C_{r,z,t}$ in the space grid corresponding to r and z at some time t, then we can obtain the photon density per unit time at the time t, denoted as $\frac{C_{r,z,t}}{2\pi r \Delta r \Delta z \Delta t}$.

4) Now that we know how the photons reaching the surface of the medium are distributed in the medium through the photon density per unit time at the time t, the classical trajectory of the photons can be got by the weight mean of the position coordinates about the photon density. For example, the photon densities are different in the z coordinates for a certain r value, thus the weight mean value of the z coordinates about the photon density for this r value is located on the classical trajectory.

The optical parameters of the media such as biological tissues are complicated and distinct significantly[17]. Here the optical parameters we used are similar to that of human breast[18], i.e., the refractive index $n = 1.55$, scattering coefficient $\mu_{\rm s} = 150$ cm^{-1}, anisotropy factor $g = 0.9$, absorption coefficient $\mu_{\rm a} = 0.035$ cm^{-1}. The structures of the biological materials which we often deal with can be usually modeled into two cases: the infinite slab of media and the semi-infinite half-space media[19], which means that the x and y coordinates extend to infinity and the z coordinates have some finite value for the infinite slab or extend to infinity for the semi-infinite media. The results of the two kind structures are given out. For the infinite slab with its thickness (the z coordinates) $d = 1.5$ cm, we should know the classical trajectories of the photons emitting out of the up and down surface of the medium, but for another case, we only need to know the path of the photons out of the up surface of the medium. The total number of the traced photons is 1.5×10^5 for each MC simulation.

Figure 2 presents classical paths for the slab at different instant t. And the classical paths for the semi-infinite half-space medium are shown in Fig. 3. The two figures show that the photons propagate more deeply and farther away while more time lapses. On the other hand, it is clear that the paths of photons from the up surface of the slab medium are affected by the down surface when the lapsing time is long. For example, the paths at the instant of 4 ns in Figs. 2 and 3 are different from each other. For the semi-infinite half-space media, all the

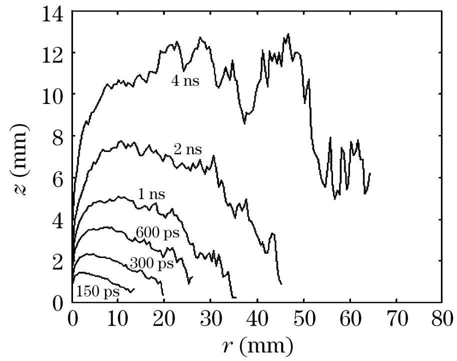

Fig. 3. Classical paths for the semi-infinite half-space medium. $n = 1.55$, $\mu_{\rm s} = 150$ cm^{-1}, $g = 0.9$, $\mu_{\rm a} = 0.035$ cm^{-1}.

entering photons finally would re-emit out of the up surface of the media; but for the infinite slab, there is some part of the entering photons emitting out of the down surface of the media. So the photon paths would penetrate deeper for the semi-infinite half-space media and shallower for the finite slab at the same instant, if the lapsing time is long enough to reach the down surface of the infinite slab media.

Figure 4 shows the influences of the anisotropy factor g on the classical path. It expresses that when g is small, it would spend more time for photons to reach the depth of the medium compared with the result in the case of larger g. Because the anisotropy factor g is the average cosine of the single scattered angle, for instance, the case of $g = 1$ embodies the forward scattering, $g = 0$ the isotropic scattering, and $g = -1$ the backward scattering, so it is apparent that the larger the g, the deeper the photons penetrate and the farther away from the entry position the photon paths reach the surface of the media.

Figure 5 shows that the scattering coefficient $\mu_{\rm s}$ influences the classical path dramatically. If the scattering coefficient is smaller, i.e., the mean scattering path length (the inverse of the scattering coefficient) should be longer, and then photons are scattered after longer distance travel. As a result, the classical paths penetrate through the medium of smaller $\mu_{\rm s}$ to reach the deeper and farther location. The parameters except for the scattering coefficient are the same for the two cases in Fig. 5, the numbers of scattering interactions in one photon path are the same but the locations of scattering interactions are different due to the different mean

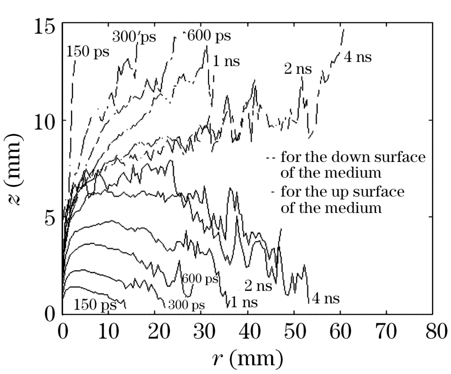

Fig. 2. Classical paths for the slab medium. $n = 1.55$, $\mu_{\rm s} = 150$ cm^{-1}, $g = 0.9$, $\mu_{\rm a} = 0.035$ cm^{-1}, $d = 1.5$ cm.

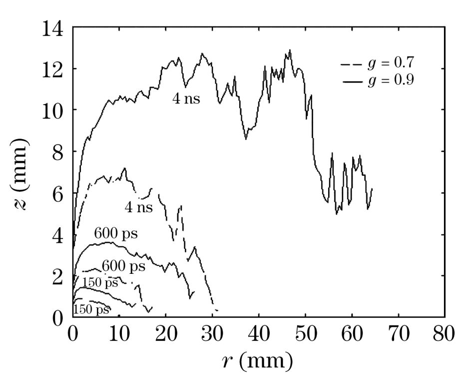

Fig. 4. Influence of the anisotropy factor g on the classical path. $n = 1.55$, $\mu_{\rm s} = 150$ cm^{-1}, $\mu_{\rm a} = 0.035$ cm^{-1}.

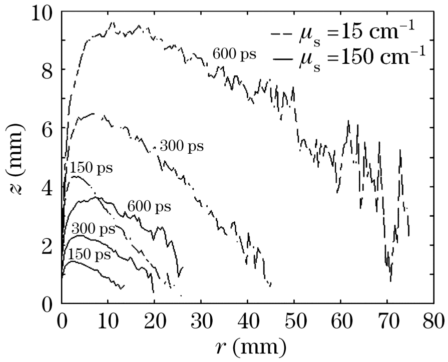

Fig. 5. Influence of the scattering coefficient μ_s on the classical path. $n = 1.55$, $g = 0.9$, $\mu_a = 0.035$ cm^{-1}.

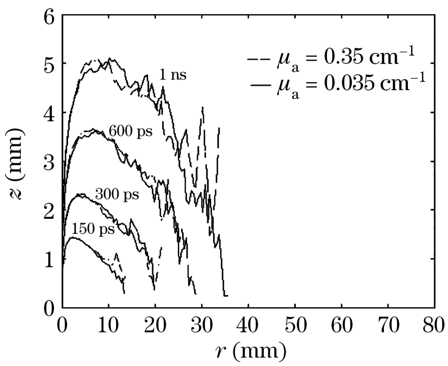

Fig. 6. Influence of the absorption coefficient μ_a on the classical path. $n = 1.55$, $\mu_s = 150$ cm^{-1}, $g = 0.9$.

scattering path lengths. This situation can be explained in the similar way to the scaling method in Monte Carlo simulation[5,20].

As can be seen in Fig. 6, the absorption coefficient μ_a has no effect on the classical paths except for statistical undulation of MC method. Thus we can describe the propagation of the photon by use of two parameters, the photon weight and the no-absorption photon path[9]. This provides new pictures of photon migration[21]. With a view to the new picture, the important parameters we want to know are the number of scattering interactions in one photon path.

In summary, we have developed an efficient method of Monte Carlo simulation to find the classical paths of photon migration in turbid media. Through introducing the grids in the time dimension, we have better understanding of time-space characteristics of photon migration. Although photons arriving at the surface seem to propagate randomly in turbid media, the classical path can be obtained from the concept of the photon density at one instant t. Here a curved classical path in turbid media plays the role of the straight photon trajectories of geometrical optics in transparent media. The physical picture of classical paths offers a more diagrammatic approach to better understand the photon migration. It can be definitely decided by photon weight and no-absorption photon path. We can diagrammatically analyze the influence of optical parameters of media on photon migration by use of classical paths. In addition, the concept of classical paths and its realization through MC simulation provide a new insight into problems of photon migration in turbid media.

This work was done during the postdoctoral period in Shanghai Institute of Optics and Fine Mechanics, Chinese Academy of Sciences.
J. Wang's present address: Britton Chance Center for Biomedical Photonics, Huazhong University of Science and Technology, Wuhan 430074. J. Wang's e-mail address is wangjiangang@mail.hust.edu.cn.

References

1. A. Ishimaru, Appl. Opt. **28,** 2210 (1989).
2. S. R. Arridge, M. Schweiger, M. Hiraoka, and D. T. Delpy, Med. Phys. **20,** 299 (1993).
3. R. F. Bonner, R. Nossal, S. Havlin, and G. H. Weiss, J. Opt. Soc. Am. A **4,** 423 (1987).
4. B. C. Wilson and G. Adam, Med. Phys. **10,** 824 (1983).
5. R. Graaff, M. H. Koelink, F. F. M. de Mul, W. G. Zijlstra, A. C. M. Dassel, and J. G. Aarnoudse, Appl. Opt. **32,** 426 (1993).
6. L. V. Wang, J. Opt. Soc. Am. A **15,** 936 (1998).
7. Y. Luo, H. Cui, X. Gu, R. Liu, and K. Xu, Chin. Opt. Lett. **3,** 659 (2005).
8. H. Tian, Y. Liu, L. Wang, X. Zhang, and Z. Gao, Chin. Opt. Lett. **4,** 105 (2006).
9. L. T. Perelman, J. Wu, I. Itzkan, and M. S. Feld, Phys. Rev. Lett. **72,** 1341 (1994).
10. L. T. Perelman, J. Wu, Y. Wang, I. Itzkan, R. R. Dasari, and M. S. Feld, Phys. Rev. E **51,** 6134 (1995).
11. L. T. Perelman, J. Winn, J. Wu, R. R. Dasari, and M. S. Feld, J. Opt. Soc. Am. A **14,** 224 (1997).
12. M. J Wilson and R. K. Wang, J. Phys. B: At. Mol. Opt. Phys. **34,** 1453 (2001).
13. A. Ya. Polishchuk and R. R. Alfano, Opt. Lett. **20,** 1937 (1995).
14. J. Zhou and J. Bai, Opt. Eng. **41,** 2577 (2002).
15. M. Testorf, U. Österberg, B. Pogue, and K. Paulsen, Appl. Opt. **38,** 236 (1999).
16. L. Wang, S. L. Jacques, and L. Zheng, Computer Methods and Programs in Biomedicine **47,** 131 (1995).
17. W.-F. Cheong, S. A. Prahl, and A. J. Welch, IEEE J. Quantum Electron. **26,** 2166 (1990).
18. A. Yodh and B. Chance, Phys. Today, **34,** (March 1995).
19. S. R. Arridge, M. Cope, and D. T. Delpy, Phys. Medicine and Biology **37,** 1531 (1992).
20. Q. Liu and N. Ramanujam, J. Opt. Soc. Am. A **24,** 1011 (2007).
21. J. Wu, J. Opt. Soc. Am. A **14,** 280 (1997).